ELSEVIER

PII: S0032-3861(97)00440-0

Polymer Vol. 39 Nos. 6–7, pp. 1279–1287, 1998

0032-3861/97/$17.00+0.00

Probing the gelation of polyvinylalcohol-water-glutaraldehyde within a porous material by ^{1}H n.m.r. — a preliminary investigation

E. W. Hansen[a,*], Kjell Olafsen[b], Thore M. Klaveness[b] and Per Olav Kvernberg[c]
[a]*SINTEF Applied Chemistry, P.O. Box 124 Blindern, N-0314 Oslo, Norway*
[b]*SINTEF Materials Technology, P.O. Box 124 Blindern, N-0314 Oslo, Norway*
[c]*UiO, P.O. Box 1033 Blindern, N-0314 Oslo, Norway*
(Revised 8 May 1997)

Proton n.m.r. relaxation times (T_1, T_2), chemical shift and line width of the solvent water protons in a polyvinylalcohol (PVA)-glutaraldehyde-water solution confined in a porous material (glass beads) revealed no significant changes during crosslinking and gel formation. Also, the self-diffusion coefficient was constant and identical to the self-diffusion coefficient of bulk water (2×10^{-5} cm^2 s^{-1}) during the reaction. Due to the smaller self-diffusion coefficient of the polymer molecules the solvent water resonance peak could be completely removed from the spectrum by applying a pulse gradient spin-echo technique, leaving only the signal from the polymer amenable for detection. In spite of the broadening effect caused by susceptibility differences between the solid porous matrix and the confined fluid, the PVA peaks were easily resolved. The observed distribution of self-diffusion coefficients of PVA could be approximated by three single diffusion coefficients ranging from 10^{-6} to 10^{-9} cm^2 s^{-1} at 25°C. The slower diffusion coefficient was found to decrease by almost an order of magnitude during the reaction with a rate of change of approximately 3×10^{-5} s^{-1} at 80°C.

(Keywords: polyvinylalcohol; glutaraldehyde; gel)

INTRODUCTION

To control the water mobility and the water profiles in injectors, high-viscosity polymeric fluids and gels have been used, with the primary application in enhanced oil recovery[1–4]. To be successful, a pre-gel solution must provide an adequate induction period so that it can be properly placed in a fracture or porous zone prior to gel formation. In recent years interest has been focused on using biopolymers as gelation agents because of their non-toxic, environmental advantages[2].

The gelation process itself is not well understood, and a number of different experimental techniques have been used to extract information related to the mechanisms and the kinetics involved in this type of reaction system[5–7]. Hansen and Lund[8,9] showed that ^{1}H n.m.r. relaxation time measurements can be used successfully to study the kinetics of gelation processes involving paramagnetic ions (chromium). However, chromium is a rather controversial chemical due to its potential as a toxic hazard. Therefore, a non-toxic gel system composed of polyvinylalcohol (PVA) and glutaraldehyde dissolved in saline water was later investigated by Hansen and coworkers using conventional ^{1}H n.m.r. spectroscopy[10]. This reaction was investigated in bulk solution giving rise to narrow resonance lines from the reagent and product molecules which could be monitored against reaction time. Variable temperature measurements enabled both mechanistic and kinetic parameters to be extracted. This system was promising enough to merit further investigation within a porous material. However, from an n.m.r. point of view, the resonance lines from a fluid confined within a porous material might suffer from susceptibility effects, i.e. different magnetic properties between the solid porous matrix and the confined fluid might cause dramatic changes in the magnetic field strength at the solid–liquid interface, producing strong magnetic field inhomogeneities (internal gradient field). This effect increases with increasing applied magnetic field strength and might result in severe line broadening masking important spectral details. In this work ^{1}H n.m.r. was used to investigate a polymer-crossbinder-water solution confined in a porous material, with the object of identifying the n.m.r. parameter(s)—if any—that can probe the reaction kinetics within such systems. Use of realistic core materials might be hampered by potential inhomogeneities in the surface chemistry of the pores and possible contamination by iron. In order to minimize these 'uncontrollable' parameters, a porous model system composed of packed glass beads is used in this preliminary n.m.r. investigation.

EXPERIMENTAL

Materials

The reagents used in this study were Floperm 665P (PVA) from OFPG Inc., Floperm 665X1 (25% glutaraldehyde in water) from OFPG Inc., and a brine solution with a total ionic strength of 0.475. All chemicals were used as received without further purification. The pH of the solution was approximately 4.7.

The porous material was composed of Ballotini glass beads (grade 14) which were packed in 5 mm n.m.r. tubes. The pore size was estimated by Hg-porosimetry, giving a nearly Gaussian pore size distribution, centered at

* To whom correspondence should be addressed

approximately 20 μm with a width at half height of approximately 4 μm. The glass beads were cleaned with distilled water and dried at 105°C for 24 h before use.

Preparation of solution

352 μl of crosslinker was mixed with 100 g of the premade gel solution and stirred for 5 min at room temperature. No significant gelation was initiated at this temperature. The prepared gel mixture was poured into a 5 mm outer diameter n.m.r. tube, which was filled with dry glass beads to a height of approximately 20 mm. The sample was centrifuged for 5 min and the surplus fluid (above the glass beads) removed. Two identical samples were prepared. One was transferred to a water bath at 80°C for 24 h, the other sample (containing no crosslinker; glutaraldehyde) was inserted into the n.m.r. magnet and measurements initiated. All measurements were performed at 25°C if not otherwise stated in the text.

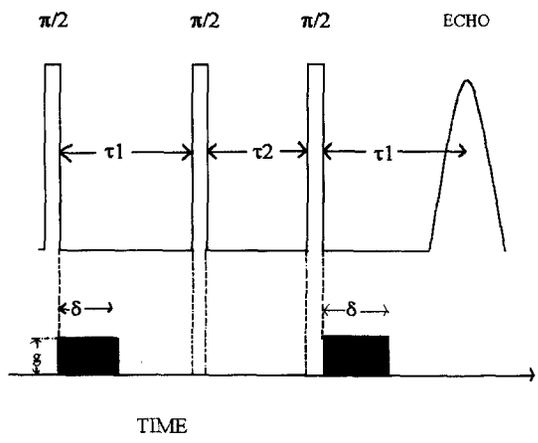

Figure 1 Schematic drawing of the pulsed field gradient stimulated echo pulse sequence

The water solvent was investigated at 300 MHz proton resonance frequency using 16 transients with a pulse separation of 10 s and a $\pi/2$-pulse of 10.5 μs. A sweep width of 10 KHz and an acquisition time of 0.05 s were used, corresponding to a digital resolution of 10 hertz per point. Line widths ($\Delta\nu$) and chemical shifts (δ) were determined by a non-linear least squares fit to a Lorentzian function. The spin-lattice relaxation time (T_1) was measured using an inversion recovery pulse sequence[11] with a time between transients of more than five times the spin-lattice relaxation time, to avoid saturation.

The spin-spin relaxation time (T_2) was measured by a Carr–Purcell–Meiboom–Gill (CPMG) pulse sequence[12] by observing the echoes between a train of π-pulses after the initial $\pi/2$-pulse. The time between π-pulses (2τ) was fixed in each experiment.

The diffusion measurements were all performed on a Bruker DMX 200 AVANCE operating at 200 MHz using a spin-lattice stimulated spin-echo pulse field gradient technique[12–14]. The pulse sequence is illustrated in *Figure 1*, showing three successive $\pi/2$ rf-pulses with a time delay of τ_1 between the first two pulses and a time delay τ_2 between the second and the last pulse. The $\pi/2$ pulse was 5.2 μs. The second part of the figure (below) shows the gradient field pulses characterized by their duration (δ) and their strength (g). The time delay between gradient pulses is denoted by Δ (not shown in *Figure 1*). The echo is observed a time τ_1 after the last rf-pulse. If not stated otherwise in the text the following parameters were used; δ = 2 ms, τ_1 = 4.5 ms, τ_2 = 135.5 ms, which gives Δ = 140 ms (when excluding the short duration of the rf-pulses). Also, the letters "a" and "b" will be used to differentiate between measured and calculated values after and before the reaction. A Bruker diffusion probe denoted MIC DIF 200 WB was used in the diffusion studies.

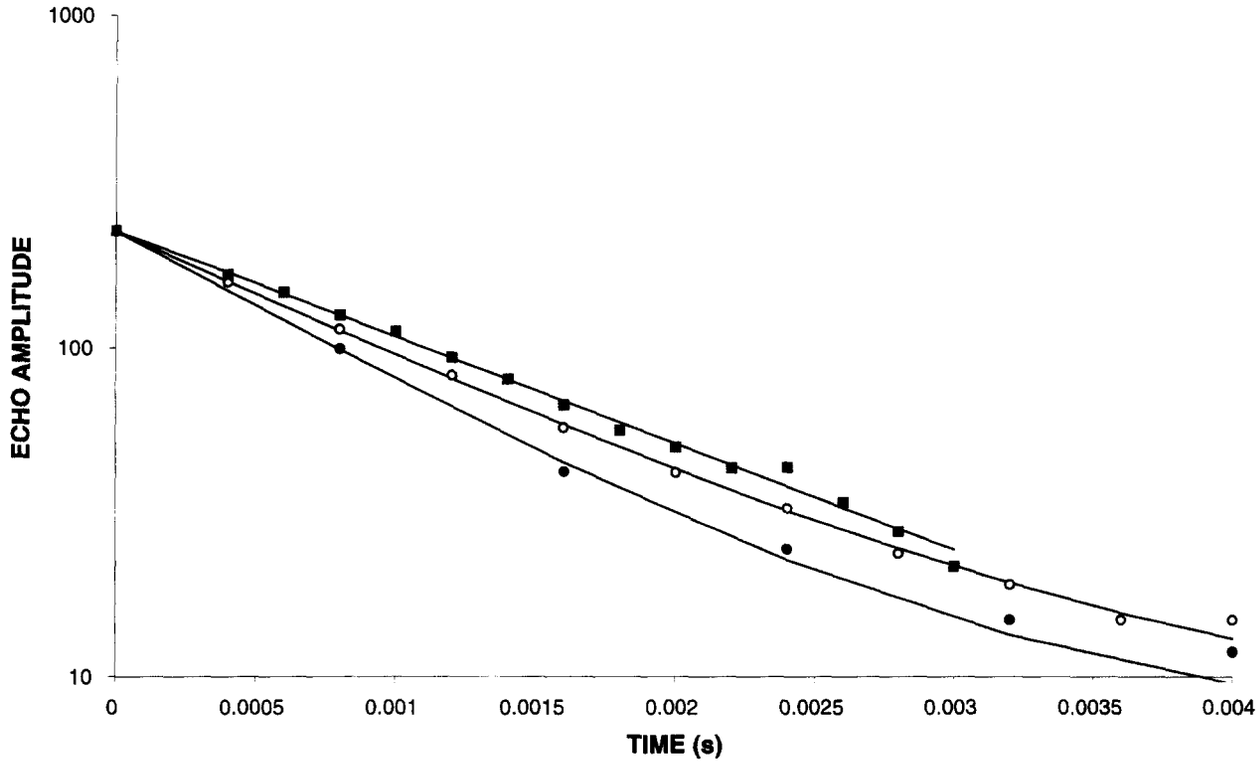

Figure 2 CPMG echo envelope curves *versus* pulse spacing $2\tau = 50$ μs (■), 100 μs (○) and 200 μs (●) and time $t = N{\cdot}2\tau$ of the water resonance peak before onset of gelation. N is the echo number

RESULTS AND DISCUSSION

Solvent water

The single pulse ^{1}H n.m.r. spectra (not shown) of the PVA-glutaraldehyde-water solution confined in glass beads revealed a single, non-resolved broad peak with no fine structure. The spectra were fitted by a Lorentzian line shape function giving $\delta^{(a)} = (4.75 \pm 0.03)$ ppm, $\Delta\nu^{(a)} = (753 \pm 15)$ Hz, $\delta^{(b)} = (4.81 \pm 0.03)$ ppm and $\Delta\nu^{(b)} = (781 \pm 20)$ Hz, indicating that these parameters are constant throughout the reaction. Note in particular the larger line width—more than two orders of magnitude larger—of the solvent water resonance peak within the porous material as compared to the line width in bulk solution. This is mainly caused by the magnetic susceptibility difference between the solid matrix (glass beads) and the confined water. This significant broadening of the water peak masks any observable resonance peaks arising from the polymer (PVA) due to its much lower concentration (1–2 mass%) and made it experimentally impossible to remove the water peak by homo-decoupling[11] or by use of any solvent suppression technique[15].

The spin-lattice relaxation time (T_1) was determined by fitting a single exponential function to the observed relaxation curve (obtained by an inversion recovery pulse sequence) giving $T_1^{(a)} = (1.618 \pm 0.010)$ s and $T_1^{(b)} = (1.660 \pm 0.003)$ s. The difference between the two values amounts to approximately 2%, and is—within experimetal error—insignificant. We also tried out an inversion recovery pulse experiment with a fixed time $\tau = T_{1,water} \cdot \ln 2$ between the π-pulse and the $\pi/2$-read pulse which would—theoretically—reduce the signal intensity of the water peak to zero. However, no signal from the polymer could be detected. This is probably due to the very small signal intensity of PVA compared to the solvent water protons, combined with broad lines resulting from some residual non-zero signal from the water protons.

For the sake of completeness, a T_2-experiment was performed using a CPMG pulse sequence with fixed inter-pulse timing (2τ) between successive π-pulses. The echo-envelope curves for the non-gelled solution are depicted in *Figure 2* for three selected inter-pulse delays ($\tau = 0.05$ ms, 0.1 ms and 0.2 ms) and show that the decay rate $1/T_{22}$ varies with the inter-pulse timing (2τ). These rates, together with the corresponding relaxation rates obtained for the gelled solution, are plotted against τ in *Figure 3* and show that the decay rate $1/T_{22}$ increases with increasing τ. This τ dependence of $1/T_{22}$ is typical of proton-containing molecules moving in a local magnetic field gradient (G). As discussed by Brown and Fantazzini[16] and Le Doussal and Sen[17] and also recently observed by Hansen *et al.*[18], the magnetic susceptibility difference between a solid matrix (glass beads) and the pore-confined fluid is the key factor responsible for the creation of this internal 'gradient' field. Le Doussal and Sen[17] have shown that under certain conditions, the decay of the CPMG echo-envelope can be written:

$$\frac{1}{T_{22}} = \frac{1}{T_2} + \frac{\gamma^2 G^2 D}{\Omega^3 \tau}[\Omega\tau - \tanh(\Omega\tau)] \qquad (1)$$

where D is the diffusion coefficient and γ the magnetogyric ratio ($2.67 \times 10^8\ s^{-1}\ T^{-1}$). Ω is a fitting parameter having the dimension s^{-1}. The fit of equation (1) to the observed data (solid curve in *Figure 3*) gave $\gamma^2 G^2 D = 1.26 \times 10^{11}\ s^{-3}$, $\Omega = 1.4 \times 10^4\ s^{-1}$ and $1/T_2 = (640 \pm 62)\ s^{-1}$. Within experimental error no significant difference could be observed in T_2 before and after heat treatment. The asymptotic value ($\tau \rightarrow \infty$ in equation (1)) of the spin-spin relaxation rate (equation (1)) corresponds to approximately half the value derived from line width measurements ($1/T_2 = \pi\Delta\nu$)[19]. We will later show that the diffusion

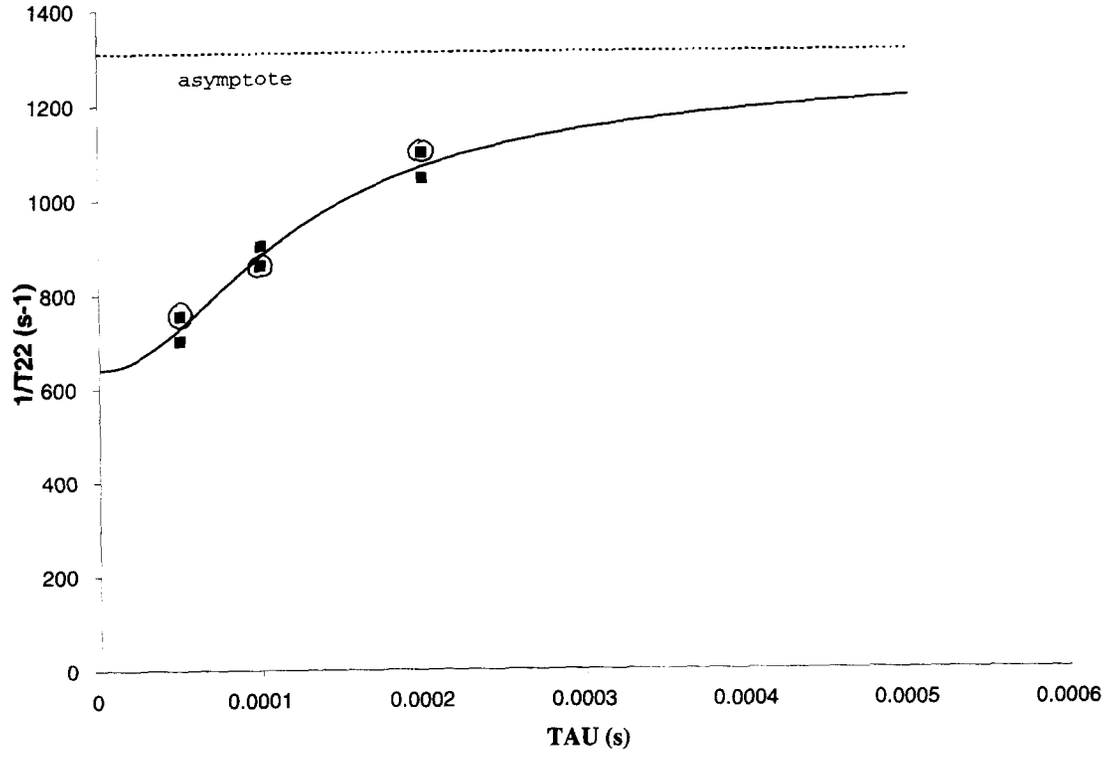

Figure 3 Apparent spin-spin relaxation rate ($1/T_{22}$) *versus* half the inter-pulse spacing (τ) from the CPMG curves in *Figure 2*. (●); before start of reaction, (■); end of reaction. The dotted line represents the asymptotic relaxation rate. The solid curve is calculated by a non-linear least squares fit of equation (2) to the observed data points

coefficient of the confined water (D) is the same as for bulk water, i.e. $D = 2 \times 10^{-5}$ cm^2 s^{-1}, which gives a value of 2.7×10^3 G cm^{-1} of the internal 'gradient' field strength. This approximate value is of the same order of magnitude as the maximum external gradient field strength which can be produced on our instrument and suggests that the pulse gradient field experiment will be hampered due to this strong internal gradient field. However, an important

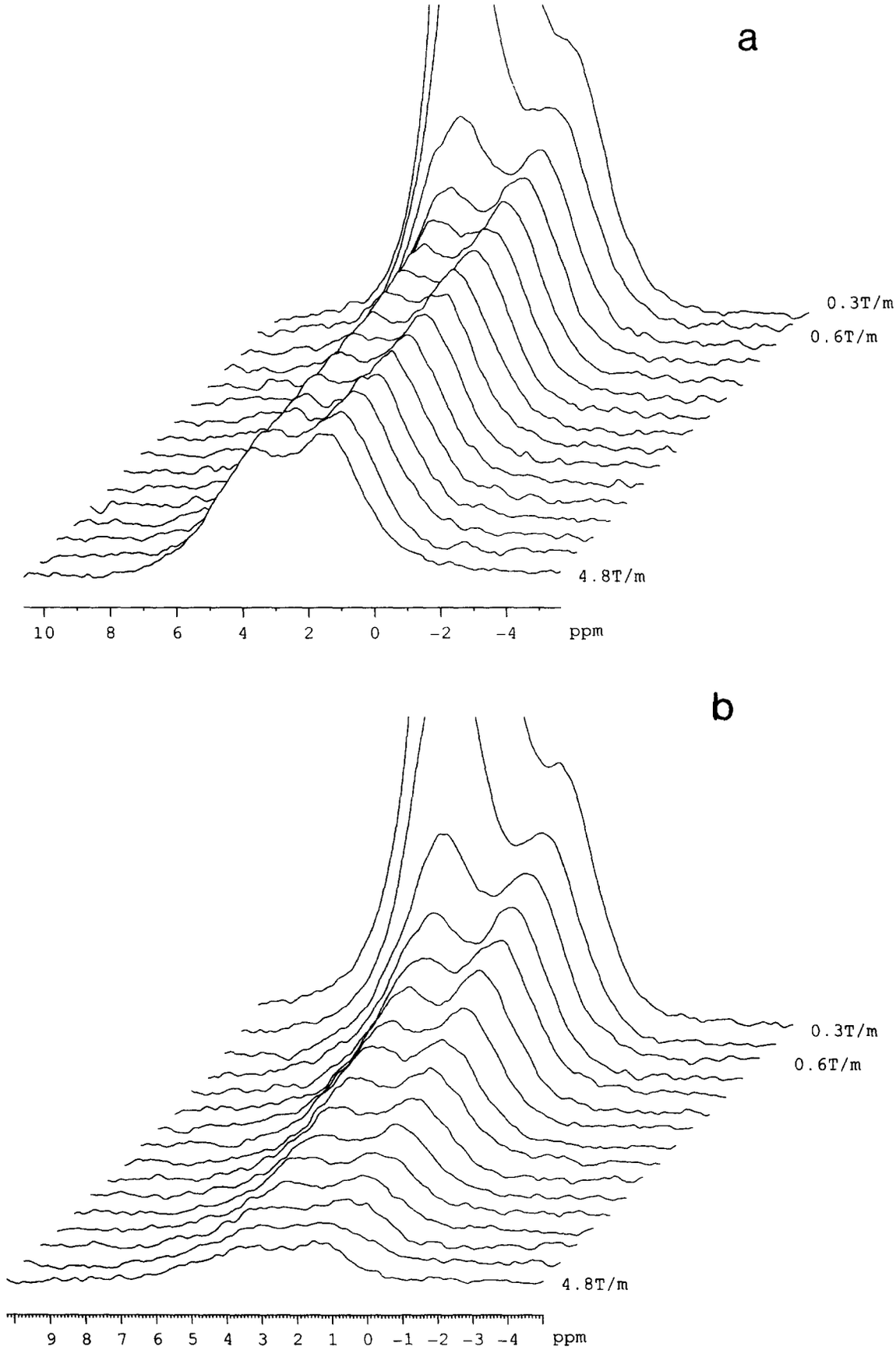

Figure 4 ^{1}H n.m.r. spectra *versus* the strength of the field gradient pulse (g) before (b) and after (a) reaction. The two resolved peaks correspond to the methine proton (low field) and the methylene protons (high field) of PVA

distinction must be kept in mind. The laboratory applied gradient field covers uniformly a range of 1–2 cm, while the susceptibility created gradient field probably covers only a few Å.

The conclusion from these experiments is that no n.m.r. parameters related to the solvent water protons changes significantly during the gel process. Thus, the gel formation itself can not be monitored by n.m.r. using the solvent water molecule as a probe molecule. These results are not unexpected considering the low concentration of polymer used in this experiment. The number of compartments or 'cells' formed during the crosslinking reaction must be relatively small, resulting in rather large compartments which are too large to affect the motional characteristics of the small solvent water molecules.

Furthermore, it is difficult—not to say impossible—to detect the n.m.r. signals from the polymer itself by applying the present n.m.r. techniques. However, keeping in mind that the diffusion coefficients of water and polymer are expected to be different, and that the diffusion of the polymer molecules is expected to decrease during crosslinking and gelation, we are left with trying out the pulse field gradient technique.

PVA

In order to understand the potential use of this technique in probing the gelation process we present the theoretical expression (equation (2)) relating the echo signal intensity (I) to the gradient field strength (g), the gradient pulse delay (δ), the time between gradient pulses (Δ) and the diffusion coefficient D when using a so-called spin-lattice stimulated echo pulse field gradient technique[13,14]. γ is the magnetogyric ratio ($2.67 \times 10^8\ s^{-1}\ T^{-1}$). The actual pulse sequence has already been discussed in the experimental section (*Figure 1*).

$$I = \sum_{i=1}^{N} A_i \cdot \exp\left[-(\gamma g \delta)^2 \cdot (\Delta - \delta/3) \cdot D_i\right] \tag{2a}$$

with

$$A_i = \frac{1}{2} M_{0i} \exp\left[-\frac{2\tau_1}{T_{2i}} - \frac{\tau_2}{T_{1i}}\right] \tag{2b}$$

Equation (2b) represents a multi-component system composed of a discrete number (N) of self-diffusion coefficients. The amplitude A_i is a function of both T_1 and T_2 (equation

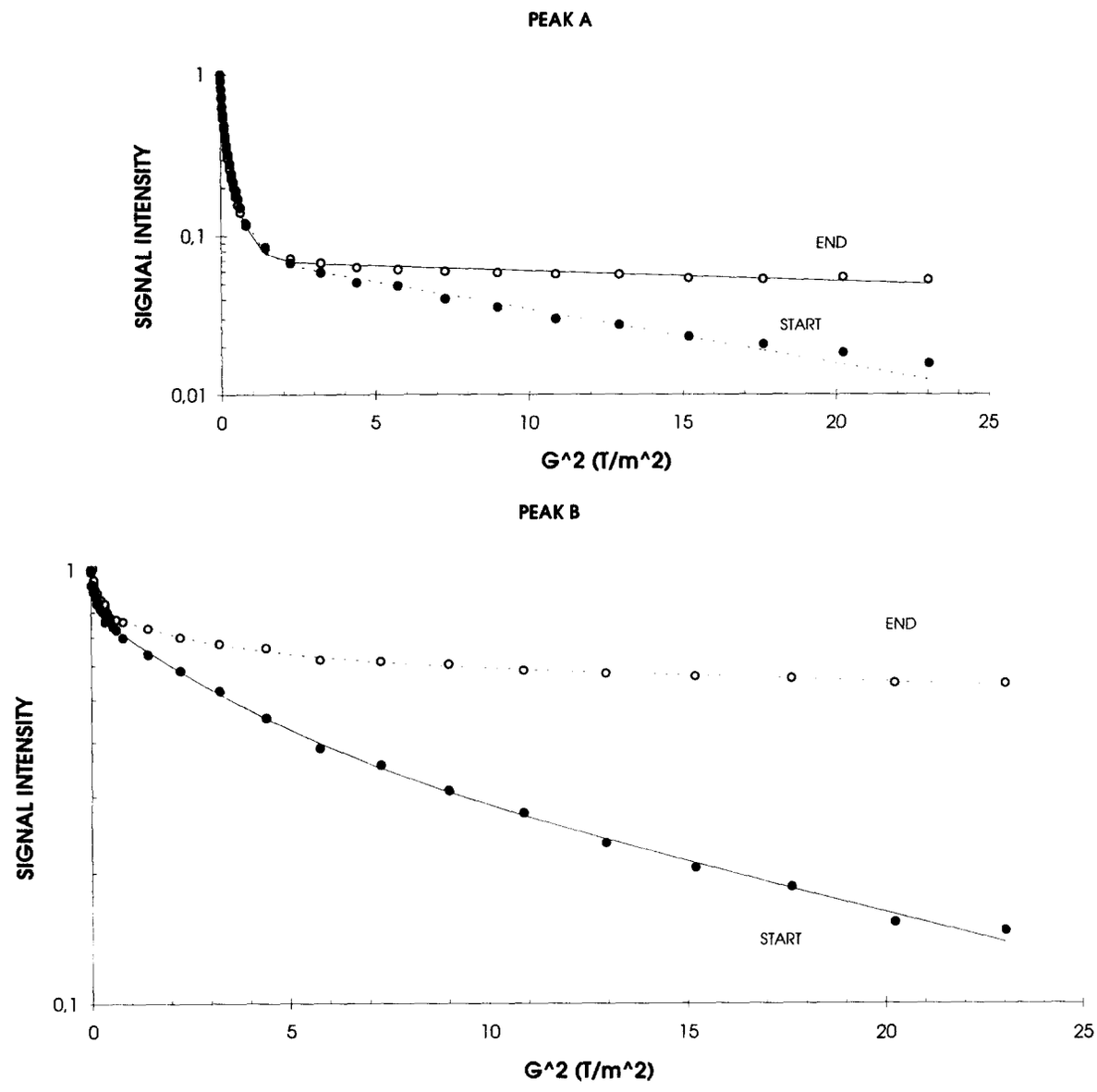

Figure 5 Echo signal intensity *versus* the square of the field gradient pulse (g^2) of the methine peak (A) and the methylene peak (B) of PVA before (start) and after (end) reaction

(2b)). M_{0i} represents the intensity of the signal. The other parameters in equation (2) have been defined previously (see *Figure 1*). The derivation of this equation is outside the scope of this work. Interested readers might consult text books or some of the references outlined in the list of references[12–14].

Figure 4 shows the Fourier transformed spectra *versus* gradient field strength (g) before and after gelation. Spectrum b was run without introducing the crosslinker (glutaraldehyde) into the solution. At large pulse gradient fields (g), two peaks can be easily observed, corresponding to the methine protons (low field) and the methylene protons (high field) of PVA. For small gradient fields the methine peak is masked by the stronger solvent water peak. The decay of the echo amplitude *versus* pulse gradient field strength is seen to be faster at the start of the reaction compared to the end of the reaction.

The numerical values of the echo amplitude (area) *versus* the square of the gradient field strength (g^2) are depicted in *Figure 5*. Peak A represents the methine proton resonance and peak B represents the methylene protons resonance. For a single diffusion component, equation (2) predicts a linear behavior of the logarithm of the echo intensity *versus* the gradient field strength squared (g^2), which can only be approximated for larger gradient field strengths. This observation suggests that the system is characterized by a distribution of diffusion modes, which is not unexpected since the molecular weight (unknown) of the polymer is known to be characterized by a distribution, as well. In order to simplify the analysis we will assume that the distribution of diffusion coefficients can be represented by a finite number (N) of diffusion coefficients (D_i) with $i = 1$–N. Equation (2) is fitted to the observed data by a non-linear least squares technique and a statistical validity test used to determine the optimum number of components (N). The results are shown in *Table 1*. Moreover, diffusion experiments performed on two different non-gelled samples signifies good reproducibility (columns 2–3 and columns 4–5 in *Table 1*).

Peak A contains an additional fast diffusion component of approximately 2×10^{-9} cm^2 s^{-1} which is not observed in peak B. The value of this diffusion coefficient does not change during the reaction and has the same value as the diffusion coefficient of bulk water. We thus tentatively assign this component to the pore confined water. The reason for not observing this component in peak B is that the chemical shift of the water peak is expected to be on the low field side of PVA, close to the methine resonance (peak A). The overlap with peak B must therefore be only marginal since it can not be singled out from the curve-fitting analysis just outlined.

The diffusion coefficients of components 2 and 3 of peaks A and B before and after gelation are—within experimental error—identical. However, the slower diffusing component (component 1, *Table 1*) of both peaks A and B reveals a significant decrease in the self-diffusion coefficient of nearly an order of magnitude as compared to the start of the reaction. The exact reason for the lack of any observable change in the derived diffusion coefficients of peaks 2 and 3 is not known. It might be, however, that the model of discretizing the echo-amplitude into a finite number of diffusion coefficients and comparing each individual diffusion coefficient before and after gelation represents an incorrect or insufficient physical picture of the overall process. A better approach would probably be to implement a distribution of diffusion coefficients (for instance a log-normal distribution) and to compare the average diffusion coefficients derived from such a distribution before and after gelation. For instance, as seen from the data in *Table 1*, the relative intensities of the 3 components of peak B change during gelation, although only the diffusion coefficient of peak 1 seems to change. An expected distribution of molecular weight of the dissolved polymer would justify such an approach, i.e. implementing a distribution of diffusion coefficients. However, this is beyond the object of this preliminary work and will be the subject for future studies.

Gelation experiment

Figure 6 shows a number of echo signal intensities *versus* the square of the field gradient pulse (g^2) and *versus* reaction time of the PVA-glutaraldehyde-water solution confined in glass beads at 80°C, *in situ*. Peak A is the methine resonance peak and peak B is the methylene resonance peak of PVA. Each of the six curves represents a single pulse field gradient experiment at a certain time during the reaction, which from bottom to top, corresponds to $t = 0.25$ h, 8 h, 14 h, 16 h, 19 h and 22 h, respectively. The diffusion coefficients of the three components of peak B (*D1*, *D2* and *D3*) were derived by a non-linear least squares procedure and the results shown in *Figure 7*. The solid curves represent single exponential fits to the observed data points with a decay rate

Table 1 Intensities and translational self-diffusion coefficients of the methine protons (A) and the methylene protons (B) derived by fitting the observed data in *Figure 6* to equation (2). Measurements are performed at room temperature (25°C)

	Before $A_i^{(1)}$ *	Reaction (b) $D_i^{(1)}$, m^2 s^{-1}	Before $A_i^{(2)}$ *	Reaction (b) $D_i^{(2)}$, m^2 s^{-1}	After A_i *	Reaction (a) D_i, m^2 s^{-1}
PEAK A (CH) component						
1	0.07 ± 0.01	$(2.8 \pm 0.2) \times 10^{-12}$	0.07 ± 0.01	$(2.8 \pm 0.2) \times 10^{-12}$	0.07 ± 0.02	$(5.2 \pm 0.7) \times 10^{-13}$
2	0.37 ± 0.04	$(8.8 \pm 0.8) \times 10^{-11}$	0.37 ± 0.03	$(9.2 \pm 0.6) \times 10^{-12}$	0.38 ± 0.03	$(9.4 \pm 0.5) \times 10^{-12}$
3	0.43 ± 0.03	$(3.4 \pm 0.4) \times 10^{-10}$	0.42 ± 0.02	$(3.6 \pm 0.3) \times 10^{-10}$	0.41 ± 0.02	$(3.7 \pm 0.4) \times 10^{-10}$
4	0.13 ± 0.02	$(2.5 \pm 0.5) \times 10^{-9}$	0.14 ± 0.02	$(2.1 \pm 0.4) \times 10^{-9}$	0.14 ± 0.02	$(2.1 \pm 0.4) \times 10^{-9}$
PEAK B(CH_2) component						
1	0.46 ± 0.08	$(1.8 \pm 0.3) \times 10^{-12}$	0.46 ± 0.06	$(1.8 \pm 0.3) \times 10^{-12}$	0.56 ± 0.02	$(2.2 \pm 0.9) \times 10^{-13}$
2	0.37 ± 0.07	$(1.1 \pm 0.3) \times 10^{-11}$	0.33 ± 0.05	$(1.1 \pm 0.2) \times 10^{-11}$	0.17 ± 0.02	$(1.3 \pm 0.4) \times 10^{-11}$
3	0.18 ± 0.02	$(2.2 \pm 0.4) \times 10^{-10}$	0.22 ± 0.01	$(3.1 \pm 0.3) \times 10^{-10}$	0.27 ± 0.01	$(2.8 \pm 0.3) \times 10^{-10}$

* The sum of peak intensities ($\sum_{i=1}^{N} A_i^{(q)}$) for each set has been normalized to 1

of $k1 = (3.86 \pm 0.85) \times 10^{-5}\ s^{-1}$ (component 1) and $k2 = (5.5 \pm 1.5) \times 10^{-5}\ s^{-1}$ (component 2), respectively. The faster diffusion component (*D3*) did not show any change in diffusion rate during the reaction. Within experimental error, the change in diffusion rate *versus* reaction time of the two slower diffusing components are the same. The decrease in diffusion coefficients *versus* reaction time is ascribed to a decreasing mobility of the polymer, tentatively explained by an increase in the effective molecular weight due to crosslinking and gelation.

Other parameters which are expected to change during gelation are the proton spin relaxation times (T_1 and T_2). We have measured the spin-lattice relaxation time of the slower diffusing component (*D1* in *Figure 7*) at the start and at the end of the reaction by applying the stimulated spin-echo pulse sequence with variable time τ_2 at a fixed pulse gradient field strength ($g = 400$ G cm^{-1}). The results are shown in *Figure 8*. The solid and dotted curves represent single exponential fits to the observed data points resulting in $T_1^{(start)} = (67.4 \pm 3.4)$ ms and $T_1^{(end)} = (169 \pm 9)$ ms.

If the signal intensity paramter M_{01} of component 1 (see equation (2)) does not change during the gel reaction we would expect the observable intensity A_1 to vary with T_1 according to equation (2). Inserting numerical values of τ_2 (=135.5 ms) and the spin-lattice relaxation times $T_1^{(start)}$ and $T_1^{(end)}$ we would expect an increase in A_1 by a factor of approximately 3.5 which is supported by the observed value of A_1 *versus* reaction time (*Figure 9*).

We would like to emphasize that the experimental parameters used in this study are by no means optimized regarding sensitivity. A change of the time parameters τ_1 and τ_2 from knowledge of the relaxation times during the reaction might improve this significantly. Decreasing the

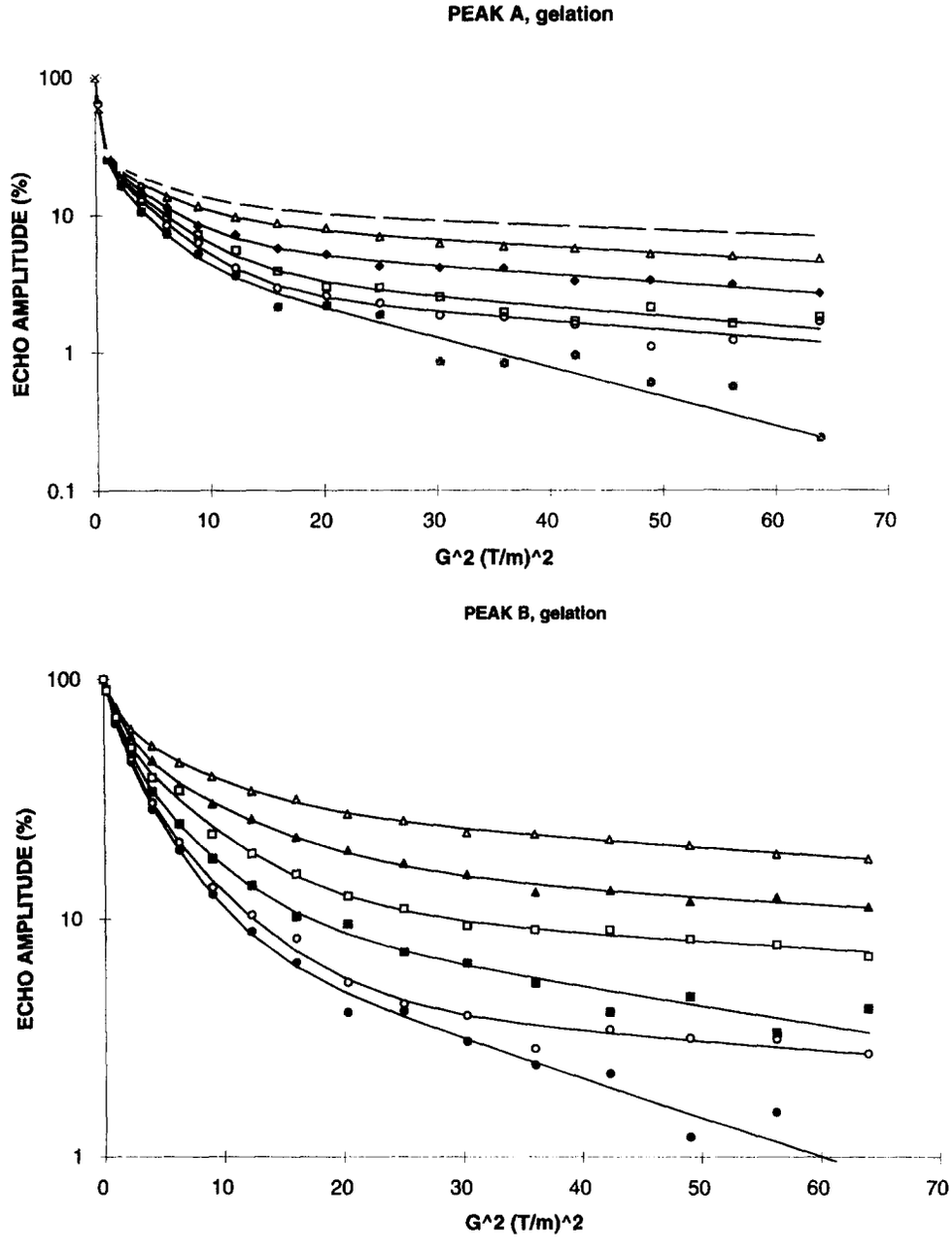

Figure 6 Echo signal intensity *versus* the square of the gradient pulse (g^2) at different times during the reaction of the methine peak (A) and the methylene peak (B). The time of acquisition of the different curves were from bottom to top $t = 0.25$, 8, 14, 16, 19 and 22 h

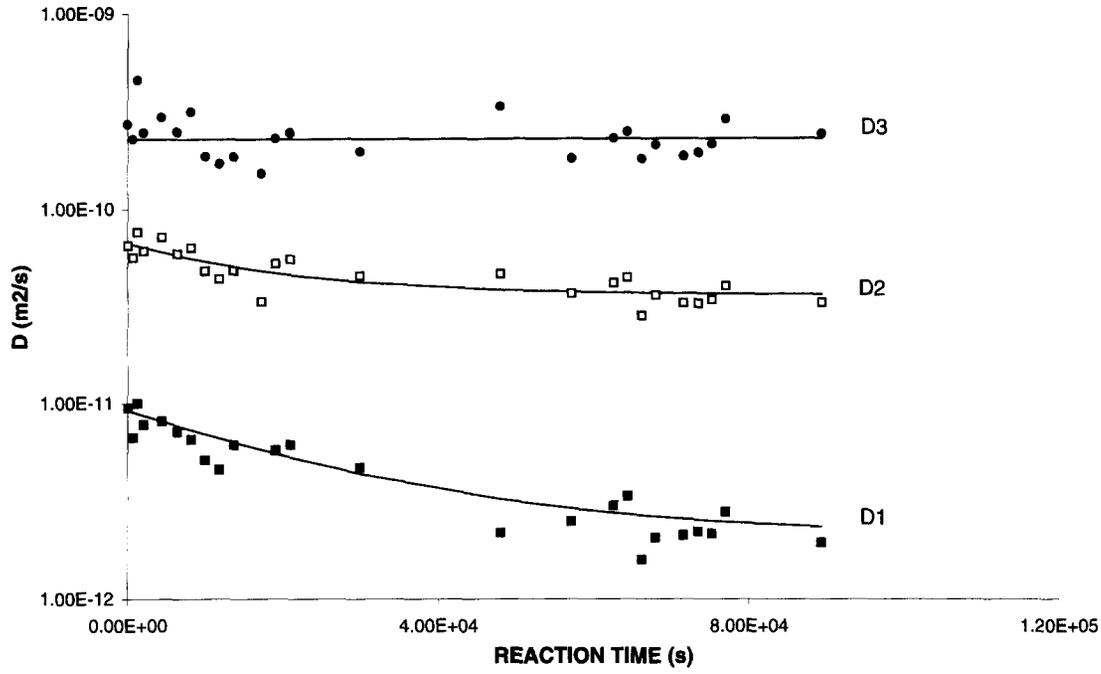

Figure 7 The self-diffusion coefficient (D_i) *versus* reaction time for the three resolved components ($i = 1$–3) of the methylene protons of PVA at t = 80°C

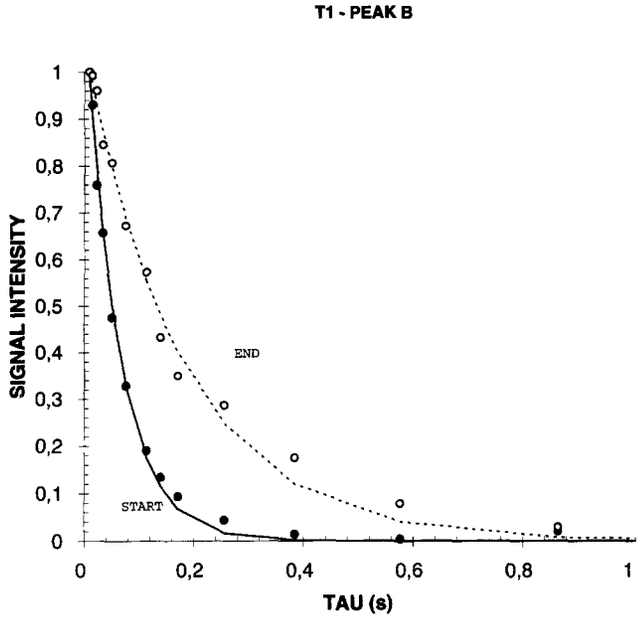

Figure 8 Signal intensity *versus* time (τ_2) obtained from the stimulated spin-echo sequence at a fixed gradient field strength of $g = 400$ G cm^{-1} at room temperature before (start) and after (end) reaction of the methylene protons of PVA

time parameter τ_2 will effectively attenuate the effect of the spin-lattice relaxation time and render a more direct estimate of M_{0i}. Also, an estimate of the self-diffusion coefficient can be improved by using an increasing number of gradient pulses. For instance, the estimation of the longer self diffusion coefficients obtained in this work is based on approximately six gradient pulses only. Likewise, increasing the number of transients will improve the sensitivity as well.

CONCLUSION

Probing the crosslinking of a polymer-crosslink-water system indirectly through changes in the n.m.r. characteristics of the solvent water protons is unsuccessful, at least when applying such a small concentration of polymer as in this work.

In spite of the significant line broadening caused by internal field gradients, originating from susceptibility differences between the solid matrix and the pore confined fluid, the pulse field gradient spin-echo technique enables the polymer peak to be resolved and monitored *versus* reaction time. The internal distribution of self-diffusion coefficients of PVA is shown to be approximated by three diffusion coefficients, each of which can be followed during the reaction. The diffusion coefficient is shown to decrease by nearly an order of magnitude with a rate of change during reaction of approximately 3×10^{-5} s^{-1}. This technique should be of general applicability in the characterization of gel forming reactions of polymer-crosslinker-water systems confined in porous media.

ACKNOWLEDGEMENT

We would like to thank NFR, Norsk Hydro, Total, Schlumberger, Dyno, Saga and Borregaard and Akzo-PQ for financial support, and Prof. Bjørn Pedersen at the UiO for permitting us to perform the diffusion measurements.

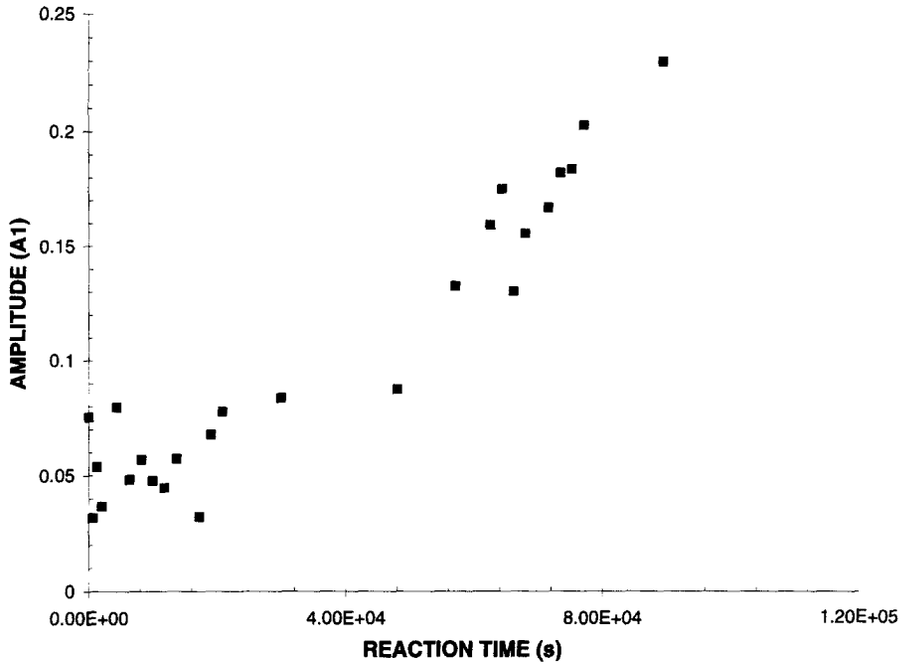

Figure 9 The amplitude $A_1 = \frac{1}{2}M_{01}\exp\left[-\frac{2\tau_1}{T_{21}} - \frac{\tau_2}{T_{11}}\right]$ of the long diffusion component of the methylene protons in PVA *versus* reaction time at t = 80°C

REFERENCES

1. Sorbie, K. S., Parker, A. and Clifford, P. J., *SPE Reservoir Engineering*, 1987, **August**, 281.
2. Chauveteau, G. and Kohler, N., *SPE 9295*, presented at the 1980 SPE Annual Technical Conference and Exhibition, Dallas, September 21–24.
3. Needham, R. B., Threlkeld, C. B. and Gall, J. W., *SPE 4747*, presented at the Improved Oil Recovery Symposium of the SPE of AIME, Tulsa, OK, April 22–24 1974.
4. Batycky, J. P., Maini, B. B. and Milosz, G., *SPE* 6th International Symposium On Oilfield and Geothermal Chemistry, Dallas, TX, January 25–27 1982.
5. Prud'homme, R. K., Uhl, J. T., Poinsatte, J. P. and Halverson, F., *SPEJ Soc. Pet. Eng. J.*, 1983, **23**, 804.
6. Prud,homme, R. K., Uhl, J. T., Poinsatte, J. P. and Halverson, F., *SPEJ Soc. Pet. Eng. J.*, 1984, **24**, 121.
7. Lund, T., Smidrød, O., Stokke, B. T. and Elgsaether, F., *Carbohydr. Polym.*, 1988, **8**, 245.
8. Hansen, E. W. and Lund, T., *J. Phys. Chem.*, 1991, **95**, 341.
9. Hansen, E. W. and Lund, T., *J. Phys. Chem.*, 1995, **99**, 1995.
10. Hansen, E. W., Holm, K. H., Jahr, D. M., Olafsen, K. and Stori, Aa., *Polym.*, 1996, accepted.
11. Harris, R. K., *Nuclear Magnetic Resonance Spectroscopy, a Physical Review*. Pitman Books Limited, London, 1983.
12. Tanner, J. E., *J. Chem. Phys.*, 1970, **52**, 2523.
13. Haase, A. and Frahm, J., *J. Magn. Res.*, 1985, **65**, 481.
14. Cotts, R. M., Hoch, M. J. R., Sun, T. and Markert, J. T., *J. Magn. Res.*, 1989, **83**, 252.
15. Hore, P. J., *J. Magn. Res.*, 1983, **55**, 283.
16. Brown, R. J. S. and Fantazzini, P., *Phys. Rev. B.*, 1993, **47**, 14823.
17. Le Doussal, P. and Sen, P. N., *Phys. Rev. B.*, 1992, **46**, 3465.
18. Hansen, E. W., Schmidt, R., Stôcker and Akporiaye, D., *Microporous Materials*, 1995, **5**, 143.
19. Bloembergen, N., Purcell, E. M. and Pound, R. V., *Phys. Rev.*, 1948, **73**, 679.